ADVANCED FUNCTIONAL MATERIALS
www.afm-journal.de

Ethanol-Dispersed Polymer Nanofibers as a Highly Selective Cell Isolation and Release Platform for CD4$^+$ T Lymphocytes

Seung-Hyun Jun, Kwanghee Kim, Hyo Jin An, Byoung Chan Kim, Chung Hee Sonn, Miju Kim, Junsang Doh, Cassian Yee, Kyung-Mi Lee, and Jungbae Kim**

A novel cell isolation and release platform using electrospun polystyrene-poly(styrene-*co*-maleic anhydride) (PS-PSMA) nanofibers is presented. Ethanol treatment of PS-PSMA nanofibers, employed for the purpose of sterilization, significantly increases their inter-fiber space for both antibody conjugation and subsequent cell separation. For the selective isolation of CD4$^+$ T cells from heterogeneous mixtures of mouse lymph nodes, capture efficiencies of up to 100% are achieved while maintaining cellular integrity and viability. Once captured, CD4$^+$ T lymphocytes can also be released from the NF scaffolds, further demonstrating its potential functionality as an immune cell-supporting and releasing matrix. This is the first demonstration of lymphocyte-culture scaffolds enabling selective isolation, accommodation, and sustained release of CD4$^+$ T cells for the purpose of cell therapies.

1. Introduction

The use of cellular immune therapy, involving the *in vitro* expansion and infusion of antigen-specific T cells, has emerged as an increasingly important modality for the treatment of cancer patients.[1,2] As an initial step, the enrichment of T cell subset populations from a heterogeneous mononuclear cell source can be critical for the downstream in-vitro isolation and expansion of antigen-specific T cells.[3] Multiple methods have been devised to extract the specific subset of lymphocytes from heterogeneous cell mixtures, based on the high affinity interaction between cell-specific antigens and their monoclonal antibodies. However, most protocols rely on antibody-conjugated magnetic nanoparticles, which require tedious steps for their synthesis, functionalization, and handling.

Electrospun nanofibers have been widely used in biomedical applications such as wound healing, tissue regeneration and drug delivery due to biocompatible polymeric strands with a large accessible surface area that are highly durable, inexpensive to produce, can be easily handled, and configured in various forms (as-spun, configured mat, column, etc.).[4–8] When functionalized to selectively bind specific cell subsets, electrospun nanofibers could offer a novel cell separation strategy. Furthermore, polymeric nanofiber scaffolds provide a 3-dimensional niche-like matrix that mimics the tissue microenvironment, allowing intimate molecular cross-talk between nanofiber scaffolds and captured cells.

In the present work, we demonstrate a novel cell isolation/enrichment and support/release platform using electrospun and alcohol-dispersed polystyrene-poly(styrene-co-maleic anhydride) (PS-PSMA) nanofibers. The PS-PSMA nanofibers, allowing for surface modification and dispersion into a configuration with an expansive inter-fiber surface area, could achieve up to 100% capture efficiency for the isolation of mouse primary CD4$^+$ T lymphocytes when conjugated with cell-specific antibodies. More importantly, PS-PSMA nanofibers were found to be biocompatible and enable the sustained release of immune cells from their scaffolds into the external milieu for an extended period of time. This observation opens up a new therapeutic strategy for the enrichment of cellular subsets for immune cell therapy by employing the non-magnetic highly specific cell isolation properties of PS-PSMA nanofibers. Future potential applications of this technology include its use in *in vivo* targeted cell expansion and sustained cell delivery systems as an innovative protocol of immune cell therapies.

S.-H. Jun, H. J. An, Prof. J. Kim
Department of Chemical and Biological Engineering
Korea University
Seoul 136-713, Republic of Korea
E-mail: jbkim3@korea.ac.kr
K. Kim, C. H. Sonn, Prof. K.-M. Lee
Global Research Laboratory
Department of Biochemistry and Molecular Biology
Korea University College of Medicine
Seoul 136-713, Republic of Korea
E-mail: kyunglee@korea.ac.kr
Dr. B. C. Kim
Environment Sensor System Research Center
Korea Institute of Science and Technology
Seoul 136-791, Republic of Korea
M. Kim, Prof. J. Doh
Department of Mechanical Engineering
Pohang University of Science and Technology
Pohang, Gyeongbuk 790-784, Republic of Korea
M. Kim, Prof. J. Doh
School of Interdisciplinary Bioscience and Bioengineering
Pohang University of Science and Technology
Pohang, Gyeongbuk 790-784, Republic of Korea
Dr. C. Yee
Clinical Research Division
Fred Hutchinson Cancer Research Center, Seattle, WA 98109 USA

DOI: 10.1002/adfm.201200657

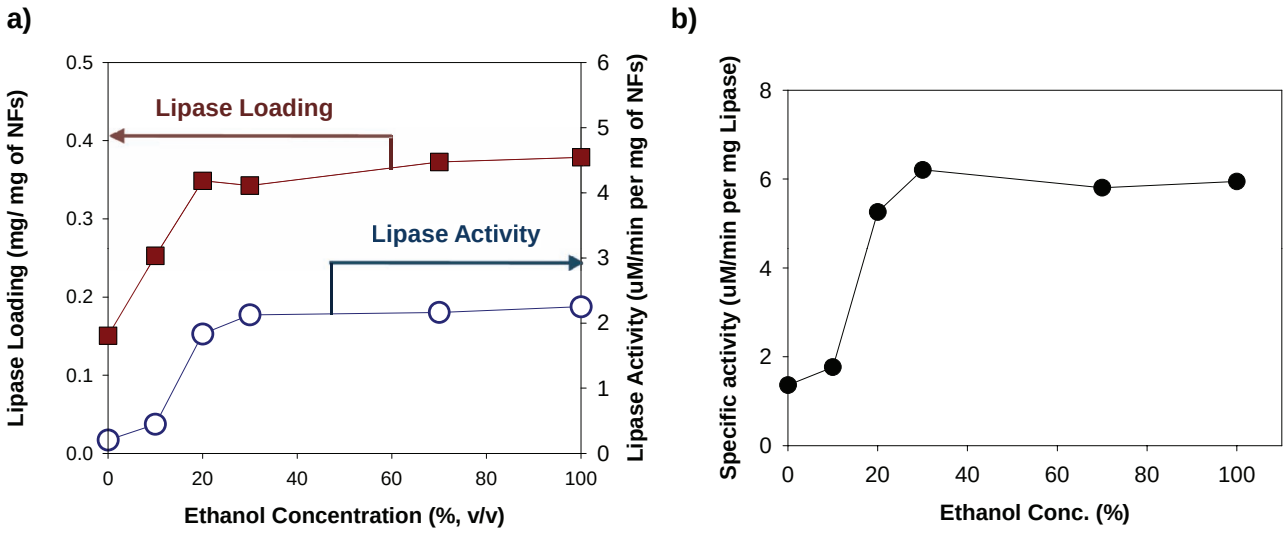

Figure 1. EtOH dispersion of PS-PSMA nanofibers and lipase immobilization. (a) The loading and activity of covelently-attached lipase onto as-spun or EtOH-dispersed nanofibers. Covalent attachment of lipase was performed by simply incubating the nanofibers in aqueous solution containing lipase. The maleic anhydride groups on PS-PSMA nanofibers react with the amino groups of lysines on the lipase molecules to form covalent linkages between nanofibers and lipase. The loading of immobilized lipase was indirectly determined by measuring the disappeared amount of lipase using the BCA assay.[27] The activity of immobilized lipase was measured by the hydrolysis of 4-nitrophenyl butyrate (4-NB) in an aqueous buffer (20 mM PB, pH 7.0). (b) Effect of EtOH concentration on the specific activity of lipase, defined as the enzyme activity per unit weight of enzyme.

2. Results and Discussion

2.1. Ethanol Dispersion of PS-PSMA Nanofibers

PS-PSMA nanofibers were chosen for the specific separation of mouse primary $CD4^+$ T lymphocytes due to several advantageous characteristics. First, the maleic anhydride groups of PSMA can react with amine groups in aqueous solution, thus facilitating the covalent attachment of antibodies without further chemical functionalization (Figure S2).[9] Second, they are insoluble in water enabling long term storage, and sufficiently durable for recycling and repeated usage.[10] Third, PS-PSMA nanofibers with the thickness of 800–850 nm can be easily prepared by simply electrospinning a homogenous mixture of PS and PSMA (weight ratio = 2: 1) in organic solvent.[11]

To improve the available surface area for the conjugation of antibodies, we first investigated the dispersion characteristics of PS-PSMA nanofibers at different concentrations of ethanol (EtOH) solution (Figure S3).[12,13] Upon EtOH treatment, as-spun nanofibers in a clumped form were dispersed into the solution, and the degree of dispersion correlated well with the EtOH concentration. PS-PSMA nanofibers, with the density of 1.05 g/cm^3, are supposed to sink in aqueous solution. However, the clumped form of as-spun nanofibers float due to entrapped air bubbles within the inter-fiber space, which can be explained by the poor contact between the water molecules and PS-PSMA nanofibers due to the strong hydrophobicity of PS-PSMA. Upon EtOH treatment, the hydrophobic nature of ethanol molecules allows for their better contact with PS-PSMA nanofibers, enabling the dispersion of nanofibers that is accompanied by the sinking of ethanol-dispersed nanofibers and removal of air bubbles.

To investigate the effect of ethanol dispersion on the biomolecule conjugation, lipase was immobilized onto both as-spun and EtOH-dispersed nanofibers (**Figure 1**a). The loading of covalently-attached lipase showed a steep increase when nanofibers were treated with solutions up to 20% EtOH, and became saturated beyond 20% EtOH. This suggests that the transfer of lipase through the nanofiber matrix was seriously limited during the lipase immobilization when the PS-PSMA nanofibers were treated by less than 20% EtOH solution. The lipase activity, measured by the hydrolysis of 4-nitrophenyl butyrate (4-NB) in an aqueous buffer, showed a similar trend to that of the lipase loading except that its saturation was observed at the EtOH concentration of 30%. Figure 1b shows the correlation between the EtOH concentration and the specific activity of lipase, defined by the lipase activity per unit weight of covalently-attached lipase, which reveals the mass transfer of substrate (4-NB) through the nanofiber matrix. Interestingly, the specific activity also showed a steep increase with the saturation at the EtOH concentration of 30%, which suggests a serious mass transfer limitation of 4-NB through the matrix of nanofibers treated by less than 30% EtOH. In summary, the ethanol dispersion of PS-PSMA nanofibers exposes more maleic anhydride groups for lipase immobilization and improves the inter-fiber space for the facile transfer of both lipase and its substrate (4-NB).

2.2. $CD4^+$ T Cell Isolation and Enrichment

$CD4^+$ T lymphocytes have been shown to exhibit clinically significant anti-tumor responses in patients with cancer,[14–16] hence $CD4^+$ lymphocytes were chosen as a primary candidate

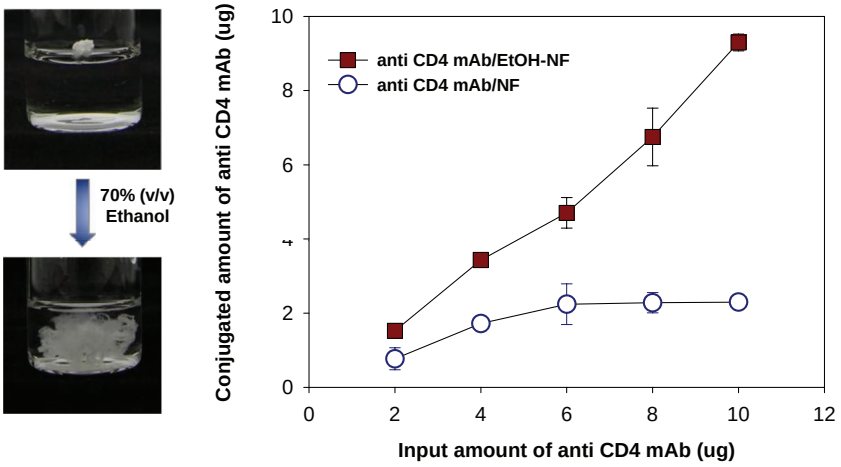

Figure 2. Conjugation of anti CD4 mAb onto as-spun nanofibers and EtOH-dispersed nanofibers. PS-PSMA nanofibers were treated by 70% EtOH solution (EtOH-NF), and used for the conjugation of anti CD4 mAb. As-spun and clumped nanofibers (NF) were used as a control. The loadings of conjugated mAb, indirectly determined by measuring the disappeared mAb from the solution using the BCA assay, are plotted as to the initial input concentration of mAb.

for the use of EtOH-dispersed PS-PSMA nanofibers as an isolation and enrichment system. Since 70% EtOH is routinely used for sterilization, we utilized 70% EtOH-dispersed nanofibers (EtOH-NF) to conjugate anti-CD4 monoclonal antibody (anti-CD4 mAb, clone GK1.5) (**Figure 2**). When the level of mAb conjugated onto nanofibers was measured, EtOH-NF demonstrated a loading capacity up to 98% of maximum in the range of 2–10 μg of input mAbs while as-spun nanofibers without EtOH-dispersion (NF) showed relatively poor conjugation at all concentrations of mAbs used. The amount of anti-CD4 mAb conjugated onto EtOH-NF was linearly correlated with the initial input concentration of anti-CD4 mAb. These results demonstrate that EtOH-NF provides a more accessible surface area for anti-CD4 mAb conjugation by enlarging their inter-fiber space.

We then examined whether anti-CD4 mAb-conjugated EtOH-NF (Ab/EtOH-NF) could selectively capture and separate mouse $CD4^+$ T lymphocytes from the heterogenous mixture of lymphocytes. For this, cells from submental, mandibular, superficial cervical, axillary, lateral axillary, inguinal, and popliteal lymph nodes of the mouse were harvested and combined to provide sufficient $CD4^+$ T lymphocytes as the starting population. These cell mixtures were incubated with Ab/EtOH-NF at 4 °C under gentle agitation, and the percentage of unbound $CD4^+$ T lymphocytes was measured after incubation for 0, 10, 20, 30, and 60 min (Figure S4). The number of $CD4^+$ T lymphocytes remaining in the solution decreased in a time-dependent manner; approximately 97% of initial $CD4^+$ T lymphocytes were found to be captured by Ab/EtOH-NF after 60 min (bottom left panel, Figure S4). When the portion of $CD4^+$ T lymphocytes captured by Ab/EtOH-NF was plotted as a function of time, more than 90% of initial $CD4^+$ T lymphocyte populations were separated from the cell mixture after 30 min incubation (bottom right panel, Figure S4). We then compared the specific separation capacity of Ab/EtOH-NF with that of non-dispersed NF conjugated with anti-CD4 mAb (Ab/NF). EtOH-NF and NF with no conjugated anti-CD4 mAb were used as controls. As shown in **Figure 3**, Ab/EtOH-NF showed almost complete removal of $CD4^+$ T cells (0.8%) after 60 min incubation while Ab/NF showed 26% of $CD4^+$ T lymphocytes still remaining under identical conditions, representing a capture efficiency of approximately 39%. Neither EtOH-NF nor NF, without conjugated anti-CD4 mAb, showed significant capturing of $CD4^+$ T lymphocytes. These data confirm the specific capability of Ab/EtOH-NF in recruiting and separating $CD4^+$ T lymphocytes from heterogeneous cell mixtures.

The difference in cell binding efficiency between non-dispersed nanofibers (Ab/NF) and EtOH-dispersed nanofibers (Ab/EtOH-NF) was further analyzed by correlating the amount of conjugated anti-CD4 mAb with the percentage of captured cells. **Table 1** summarizes the amounts of conjugated anti-CD4 mAb of Ab/NF and Ab/EtOH-NF, together with their specific cell binding capacity. Even at non-saturating doses of anti-CD4 mAb (≤ 2 μg), greater efficiency of cell-binding was observed using EtOH-dispersed vs. non-dispersed NF. Although the amount of conjugated anti-CD4 mAb on EtOH-NF was two times higher than that on NF, the capacity of specific cell binding on Ab/EtOH-NF was 3.9 times higher. These results suggest that the inter-fiber space of non-dispersed NF without EtOH treatment was not efficiently utilized for mAb conjugation, presumably due to their tightly-clumped structure, thereby limiting cell accessibility to surface-conjugated antibody. In contrast, the enlarged inter-fiber space of fully-dispersed EtOH-NF allowed for facile transfer of larger-sized cells as well as smaller-sized antibodies. The increased ratio of cell binding capacity to conjugated antibody concentration (1.93) reveals the additional contribution of enlarged inter-fiber space in relieving the mass transfer limitation to the passage of larger cells when compared to that of smaller-size antibodies.

2.3. Ethanol-Dispersed Nanofibers as an Immune Cell-Supporting and Releasing Matrix

Figures 4a and 4b show $CD4^+$ T lymphocytes bound to the surface of Ab/EtOH-NF as well as to the inner matrix of nanofiber scaffolds, demonstrating that $CD4^+$ T lymphocytes can successfully pass through inner scaffolds and bind to Ab/EtOH-NF. $CD4^+$ T lymphocytes bound onto Ab/EtOH-NFs appear intact and undamaged based on scanning electron microscope (SEM) images (Figure 4c and 4d). To determine if $CD4^+$ T lymphocytes were bound to Ab/EtOH-NFs, cell-bound NF scaffolds were stained with a biotin-conjugated anti-CD4 mAbs (clone RM4-4, eBioscience) and streptavidin-FITC targeting an epitope distinct from that used by the NF capture anti-CD4 mAb (clone GK1.5). Fluorescence was determined using epifluorescence microscopy. Stained cell-NF complexes were washed extensively overnight to quench background fluorescence. As shown

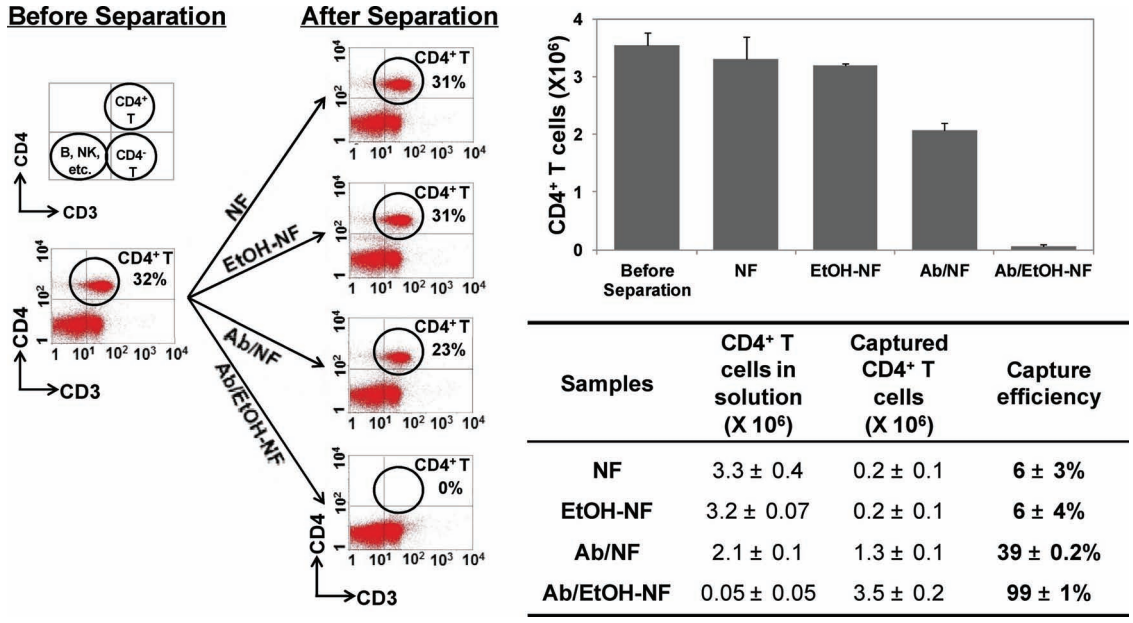

Samples	$CD4^+$ T cells in solution ($X 10^6$)	Captured $CD4^+$ T cells ($X 10^6$)	Capture efficiency
NF	3.3 ± 0.4	0.2 ± 0.1	6 ± 3%
EtOH-NF	3.2 ± 0.07	0.2 ± 0.1	6 ± 4%
Ab/NF	2.1 ± 0.1	1.3 ± 0.1	39 ± 0.2%
Ab/EtOH-NF	0.05 ± 0.05	3.5 ± 0.2	99 ± 1%

Figure 3. Isolation of $CD4^+$ T lymphocytes from the heterogeneous mixture of mouse lymph node cells using Ab/EtOH-NF scaffolds. The separation efficiency of $CD4^+$ T lymphocytes by NF and EtOH-NF conjugated with or without anti-CD4 mAbs were compared by FACs (left panels). The average $CD4^+$ T cells remaining in solution or bound to each nanofiber scaffolds were plotted as a bar graph (upper right) and presented as a table (lower right).

Table 1. Conjugated antibody amount and specific cell binding capacity of Ab/NF and Ab/EtOH-NF when the initial input of CD4 mAb was 2 μg for its conjugation onto 1 mg of nanofibers.

	Conjugated amount of CD4 mAb per 1 mg of nanofibers	Capture efficiency of $CD4^+$ T cells
Ab/EtOH-NF (A)	1.6 μg	85%
Ab/NF (B)	0.8 μg	22%
Ratio (A/B)	2.0 (C)	3.9 (D)
Ratio (D/C)	1.93	

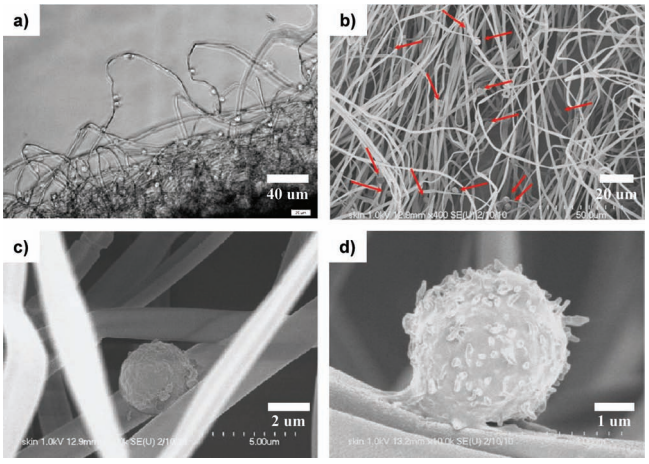

Figure 4. The microscopic images of $CD4^+$ T lymphocytes, as revealed by optical microscope and SEM. The optical microscope image (a) and SEM images (b–d) of $CD4^+$ T lymphocytes bound onto Ab/EtOH-NF are shown.

in **Figure 5**, green fluorescence of $CD4^+$ T lymphocytes could be visualized among the Ab/EtOH-NF scaffolds, and were found to overlap all DAPI (4′,6-diamidino-2-phenylindole)-stained cells. In contrast, little staining was observed among Ab-free NF (EtOH-NF), demonstrating that anti-CD4 mAbs on EtOH-NF scaffolds were able to capture $CD4^+$ T cells in a specific manner. To further confirm the viability of bound $CD4^+$ T lymphocytes on Ab/EtOH-NF, cells were double stained with DAPI and propidium iodide (PI). DAPI binds to all nuclei of the cells by passing through the intact cell membrane while PI cannot permeate through the membrane of viable cells. As a result, DAPI stains all the cells in blue, and the nuclei of dead cells are stained red. As seen in Figure 5 (bottom panel), most of the bound cells were found to be DAPI positive and PI negative, indicating that cells are viable even after selective capture and culture onto Ab/EtOH-NF. These data support the fidelity and safety of anti-CD4 mAb/EtOH-NF system as a functional lymphocyte isolation and release platform.

Interestingly, the interaction between $CD4^+$ T lymphocytes and Ab/EtOH-NF was not based on a point contact but rather by the engagement of large contact area with one dimensional length of 1–2 μm (Figure 4d). These features reveal the potential of rigorous interactions between nanofibers and cells, which may be critical for the survival and activation of $CD4^+$ T lymphocytes when transplanted *in vivo*. In keeping with this hypothesis, when the $CD4^+$ T cell-bound Ab/EtOH-NF complex was further incubated in T cell stimulating media [1 μg/ml of anti-CD3 (clone 2C11) + 1 μg/ml of anti-CD28 (clone 37.51) mAbs], a gradual release of cells into the culture media was observed over time (**Figure 6**). Furthermore, using anti-human

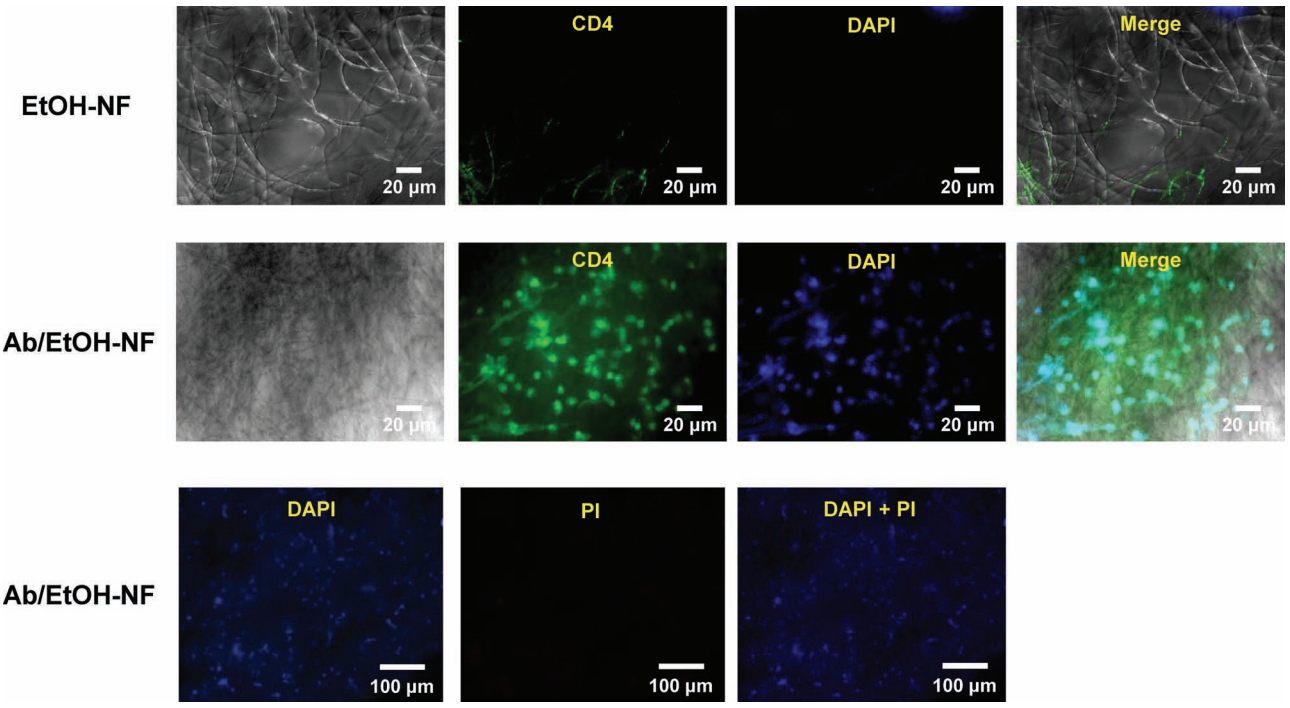

Figure 5. Fluorescence images of $CD4^+$ T lymphocytes bound on Ab/EtOH-NF. Top and middle panel, cell-bound EtOH-NF or Ab/EtOH-NF scaffolds were stained with a biotin-conjugated anti-CD4 mAbs (clone RM4-4) and streptavidin-FITC targeting an epitope distinct from that used by the NF capture anti-CD4 mAb (clone GK1.5). Fluorescence was determined using epifluorescence microscopy. Bottom panel, cell-bound Ab/EtOH-NF scaffolds were stained with DAPI, shown in blue, and PI, shown in red. No dead (red) cells were present in the $CD4^+$ T lymphocytes bound to nanofibers.

CD4 mAbs conjugated to EtOH-NF, human $CD4^+$ T cells could be isolated (Figure S5). The translation of this technology to human T cells demonstrates the potential application Ab/EtOH-NF scaffolds for use as an immune cell-supporting and releasing matrix in the development of cellular therapy.

3. Conclusions

This report demonstrates, for the first time, that a specific lymphocyte subset of immune cells, $CD4^+$ T lymphocytes, can be isolated and enriched with up to 100% purity using electrospun

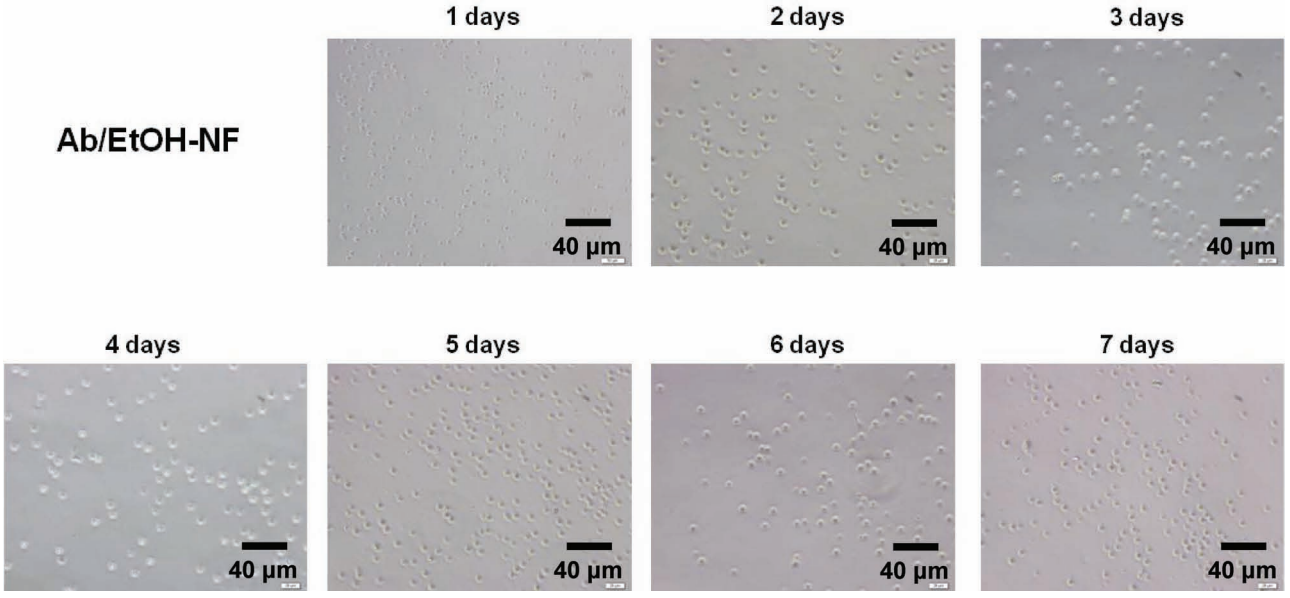

Figure 6. Time-dependent release of $CD4^+$ T lymphocytes cultured onto the Ab/EtOH-NF scaffolds. $CD4^+$ T cell-bound Ab/EtOH-NF complex was incubated with 1 μg/ml of anti-CD3 (clone 2C11) + 1mμg/ml of anti-CD28 (clone 37.51) mAbs, and the release of T cells into the culture media was monitored over time. The released cells were visualized by using an optical microscope.

PS-PSMA nanofibers conjugated with anti-CD4 mAbs. The presence of maleic anhydride groups in PS-PSMA nanofibers facilitates the conjugation of antibodies without requiring any tedious functionalization process. Furthermore, the ethanol-dispersion of PS-PSMA nanofibers greatly increased the accessible surface area of hydrophobic nanofiber mesh for the conjugation of antibody within NF scaffolds, leading to a dramatic improvement in the efficiency of $CD4^+$ T lymphocyte isolation. In addition, captured $CD4^+$ T lymphocytes in the nanofiber scaffolds could be successfully maintained and released, further demonstrating its potential functionality as an immune cell supporting/releasing matrix. Therefore, the present work introduces the application of nanofiber scaffolds as an immune cell "depot", which can house the target cells *in situ*, e.g., in tumor sites, and gradually release them to function *in vivo*.

Although we present $CD4^+$ T lymphocytes as an example, our nanofiber system can be applied to the separation of other cell types, including leukocyte subsets, tumor cells, or pluripotent stem cells, simply by changing the NF capture antibody. For example, antibodies against CD8 can be used to isolate $CD8^+$ T cells, NKp46 for NK cells,[17,18] and those against CD90, CD44, or CD105, to isolate mesenchymal stem cells.[19,20] Tumor cells can also be isolated by the nanofiber system using antibodies against tumor-specific surface antigens; e.g. HER-2/Neu for breast and ovarian cancer,[21,22] MUC-1 for breast and pancreatic cancer.[23,24]

The properties of PS-PSMA nanofibers, allowing for surface modification and dispersion into a configuration with an expansive surface area, enable highly efficient target cell capture using selective antibodies and can be readily scaled to a process with high starting cell populations (Figure S6). This platform also provides thorough and intimate contact between captured target cells and conjugated biomolecules for enhanced survival and/or activation signal delivery to cells of interest, enabling controlled and sustained cell release from the nanofiber scaffold. Furthermore, by using biocompatible materials such as PLA, PLLA, PCL, PLGA, or P(LLA-CL),[25,26] this platform can be readily translatable to *in vivo* applications where it may serve as an implantable immune cell depot at target disease sites.

4. Experimental Section

Materials: Lipase from Rhizopus oryzae, 4-nitrophenyl butyrate (4-NB), and N,N-dimethylformamide (DMF) were purchased from Sigma (ST Louis, MO, USA). Polystyrene (PS, MW = 950,400), and Poly(styrene-co-maleic anhydride) (PSMA, MW = 224,000), and tetrahydrofuran (THF) were purchased from Aldrich (Milwaukee, WI, USA). Ethanol was purchased from Deajung (Siheung, Korea). The BCA protein assay reagent kit was purchased from Pierce (Rockford, IL, USA). Anti-mouse CD3(145-2C11), CD4 (GK1.5, RM4-4), NK1.1 (PK136), and anti-human CD4 (OKT4, RPA-T4) monoclonal antibodies (mAbs) and streptavidin conjugated with or without fluorescein isothiocyanate (FITC), phycoerythrin (PE), allophycocyanin (APC) and biotin were purchased from eBioscience (San Diego, CA, USA). Anti-mouse CD19 (6D5) mAb conjugated with Peridinin Chlorophyll Protein Complex (PerCP) was purchased from BioLegend (San Diego, CA, USA). All other reagents were purchased from Sigma (ST Louis, MO, USA) or Aldrich (Milwaukee, WI, USA).

Preparation of dispersed polymer nanofibers: Polymer NFs were a blend of PS and PSMA and prepared via electrospinning, as described previously.[9,10] Briefly, the polymer solution was prepared at room temperature by dissolving 2:1 weight ratio of PS:PSMA mixture in THF. After dissolution of PS:PSMA mixture for 3 hours on the magnetic stirrer, acetone (20%, v/v) was added to decrease the viscosity of polymer solution. Then, the polymer solution was loaded into a 5 mL plastic syringe equipped with 30 gauge stainless steel syringe needle. Electrospinning was performed under the voltage of 7 kV by using a high-voltage supplier (Ormond Beach, FL, USA) and with the polymer solution fed (0.1 mL/h) using a syringe pump (PHD-2000 Infusion, Harvard Apparatus, Holliston, MA, USA). The electrospun NFs were collected on a clean aluminum foil (connected to the ground) that was placed at a suitable distance (7–10 cm) from the tip of the needle (Figure S1). A nonwoven mat form of NFs on the foil was detached by using tweezers, and stored at room temperature. Aqueous ethanol solution was used to prepare the samples of dispersed NFs. A clump of electrospun NFs (1 mg) was immersed in aqueous solutions with various ethanol concentrations (0, 10, 20, 30, 70, and 100%, v/v). The vials containing NFs in ethanol solutions were vortexed for 5 min, shaken at 200 rpm for 10 min, and shaken by hand for 30 s. After incubation in the ethanol solutions, NFs were washed for several times until alcohol was thoroughly removed from the solution. Dispersed NFs were stored in 1X phosphate buffered saline (PBS) (pH 7.4) at room temperature.

Immobilization of biomolecules on polymer nanofibers: Biomolecules, such as lipase and antibody, were immobilized onto ethanol-treated NFs (EtOH-NF) and non-dispersed NFs (NF), respectively. For the covalent attachment of lipase, a clump of NFs (1 mg) was incubated in 2 mL of 20 mM sodium phosphate buffer (PB) (pH 7.0) containing 4 mg of lipase. The glass vial containing NFs and lipase was shaken at 200 rpm for 30 min, and then placed on the rocker (50 rpm) in a refrigerator (4 °C) for 4 hours to allow for completion of covalently attachment between lipase and NFs. Lipase immobilized NFs were incubated further with 100 mM Tris-HCl (pH 7.0) for 30 min to cap the un-reacted maleic anhydride groups of NFs. Lipase immobilized NFs were washed extensively with 10 mM sodium phosphate buffer (pH 7.0), and were stored in the same buffer at 4 °C until use. For the conjugation of anti-CD4 mAb, 70% ethanol-treated NFs (EtOH-NF) and as-spun NFs were used as dispersed and non-dispersed NFs, respectively. Conjugation of anti-CD4 mAb on polymer nanofibers was performed in a similar way to that of lipase immobilization. EtOH-NF or NFs (1 mg) was incubated in 2 mL of 1X PBS (pH 7.4) containing various concentrations of anti-CD4 mAb (2–10 μg). The glass vials containing NFs and antibodies solution was shaken at 150 rpm for 30 min, and then placed on the rocker (50 rpm) in a refrigerator (4 °C) for overnight. After incubation, anti-CD4 mAb conjugated NFs (Ab/EtOH-NF) were washed with 1X PBS (pH 7.4), and the un-reacted maleic anhydride groups were capped with 50 mM Tris-HCl (pH 7.4) for 30 min. Finally, Ab/EtOH-NF were washed extensively with 1X PBS (pH 7.4), and were stored in the same buffer at 4 °C until use.

Measurements of lipase activity and biomolecule loadings: The lipase activity was measured by the hydrolysis of 4-nitrophenyl butyrate (4-NB) in 20 mM PB buffer (pH 7.0). To prepare 4-NB substrate solution, 100 μL of 20 mM 4-NB was mixed with 9.9 mL of 20 mM PB buffer (pH 7.0). Lipase-immobilized nanofibers were added to a vial containing 10 mL of 4-NB solution, and then the vials were shaken at 200 rpm. Aliquots were withdrawn time-dependently, and the absorbance at 410 nm was measured by using a spectrophotometer (Shimadzu, UV-2450, Kyoto, Japan). The lipase activity of each sample was calculated from the time-dependent increase of absorbance at 410 nm (A_{410}). The loadings of immobilized lipase and antibody were obtained by measuring the protein contents in solution before and after the biomolecule immobilization. The BCA protein assay was performed to measure the protein contents in solution, and the absorbance at 562 nm was measured using a spectrophotometer (Shimadzu, UV-2450, Kyoto, Japan).

Cell preparation and culture: Seven-week-old C57BL/6 mice were purchased from the Narabiotech (Seoul, Korea) and maintained in the Korea University Animal Facility. Mice were used at 7–10 weeks of age. All procedures were approved by Korea University Institutional Animal Care & Use Committee (KUIACUC-2009-105). Peripheral (Submental,

Mandibular, Superficial Cervical, Axillary, Lateral Axillary, Inguinal, and Popliteal) lymph nodes were excised from C57BL/6 mice. Single cell suspensions were mashed through a 70 μm nylon cell strainer (BD biosciences, San Diego, CA, USA), and cell washed in 1X PBS (pH 7.4) with 5% fetal bovine serum (FBS) (Lonza Walkersville, MD, USA). $CD4^+$ T cells on Ab/EtOH-NF were cultured in RPMI-1640 (Welgene, Deagu, Korea) supplemented with 5% fetal bovine serum, antibiotics (penicillin 100 U/ml, streptomycin 100 μg/ml), 1X NEAA (Lonza Walkersville Inc., MD, USA), 10 mM HEPES Buffer, 1 mM sodium pyruvate (Cellgro, VA, USA), 55 M 2-ME (Gibco, CA, USA), 1 μg/ml anti-CD3 (clone 2C11), and 1 μg/ml anti-CD28 (clone 37.51, eBioscience, CA, USA). The released cells into the culture media were visualized using an inverted microscope (CKX41, Olympus, Tokyo, Japan) at 1 to 7 days.

Human PBMCs isolation: Human peripheral blood mononuclear cells (PBMC) were isolated from whole blood of healthy volunteers using Ficoll-Paque (Amersham Pharmacia Biotech) following manufactures' instructions.

Flow cytometry analysis: Anti-mouse CD3 (145-2C11), CD4 (GK1.5, RM4-4), and NK1.1 (PK136) monoclonal antibodies (mAbs) conjugated with or without fluorescein isothiocyanate (FITC), phycoerythrin (PE), or allophycocyanin (APC) were purchased from eBioscience (San Diego, CA, USA). Anti-mouse CD19 (6D5) mAb conjugated with Peridinin Chlorophyll Protein Complex (PerCP) was purchased from BioLegend (San Diego, CA, USA). Isolated cells were resuspended in 100 ml of FACs buffer (PBS containing 2% FBS and 0.02% sodium azide) and incubated with anti-CD16/CD32 mAb (2.4G2, Fc block) to block FcIII/II receptors. Cells were then incubated for 20 min at 4 °C. Flow cytometry was performed with a FACScalibur (BD Bioscience, San Diego, CA, USA) and the data analyzed with Cell Quest software (BD Pharmingen, San Jose, CA, USA).[25] Fifty thousand lymphocyte populations gated by forward scatter (FCS)/side scatter (SSC) were analyzed.

Imaging of bound $CD4^+$ T cells on Ab/EtOH-NF: The images of $CD4^+$ T cells on Ab/EtOH-NF were obtained by using inverted microscope (CKX41, Olympus, Tokyo, Japan) and Field-Emission Scanning Electron Microscope (FESEM, Hitachi, S-4700, Tokyo, Japan). For the imaging with optical microscope, the samples were gently washed with PBS and fixed with 2% glutaraldehyde in phosphate buffer (pH 7.2) at 4 °C for overnight. Then, the samples were post-fixed with 1 ~ 2% osmic acid in PBS for one hour. The samples were dried at room temperature for overnight. Samples were observed under an inverted microscope. In case of SEM analysis, the samples were gently rinsed with PBS, fixed with 2% glutaraldehyde in 0.1M phosphate buffer at 4 °C for overnight, and post-fixed with 1 ~ 2% osmic acid in PBS for 1 hour. The samples were then dehydrated using a series of ethanol solutions (50%, 60%, 70%, 90%, 95%, 100%, 100%, and 100%), followed by tert-butyl alcohol for three times, and stored at 4 °C for overnight. Finally, the samples were fully dried in a freeze dryer (ES-2030, Hitachi, Tokyo, Japan). The samples were mounted onto aluminum stubs, coated with platinum using an ion coater (IB-5, Eiko, Ibaragi, Japan) before the SEM observation.[26]

Immunofluorescence staining and viability assay: For $CD4^+$ T cell visualization, samples were fixed with 4% paraformaldehyde for 10 min at RT and incubated with Biotin-anti-CD4 mAbs (RM4-4) for 3 hrs. After overnight washing, the samples were incubated with streptavidin-FITC for 1 hr and stained with DAPI. The fluorescent images were visualized using fluorescence microscopy (Axio Observer.Z1, Carl Zeiss, Germany). Cell viability was measured using fluorogenic dye assays based on the inclusion or exclusion of two fluorogenic stains, 4′,6-diamidino-2-phenylindole (DAPI) (Invitrogen, CA, USA) and propidium iodide (PI) (BD bioscience, CA, USA). The Samples were incubated with DAPI and PI for 15 min at RT in the dark, and washed 2 times. The images of cells on Ab/EtOH-NF were obtained by fluorescence microscopy (ECLIPS Ti, Nikon, Japan).

Supporting Information

Supporting Information is available from the Wiley Online Library or from the author.

Acknowledgements

S.-H.J. and K.K. contributed equally to this work. This work was supported by the National Research Foundation (NRF) grant (2011K000833), the Korea Foundation for International Cooperation of Science & Technology (KICOS) grant (K20702001994-11A0500-03610), the Converging Research Center Program (2011K000815) through the Korean Ministry of Education, Science & Technology.

Received: March 9, 2012
Revised: May 2, 2012
Published online: June 25, 2012

[1] A. Mackensen, N. Meidenbauer, S. Vogl, M. Laumer, J. Berger, R. Andreesen, *J. Clin. Oncol.* **2006**, *24*, 5060.
[2] Z. Liu, S. Tian, L. D. Falo Jr., S. Sakaguchi, Z. You, *Mol. Ther.* **2009**, *17*, 1274.
[3] C. Yee, *J. Transl. Med.* **2005**, *3*, 8.
[4] C. P. Barnes, S. A. Sell, E. D. Boland, D. G. Simpson, G. L. Bowlin, *Adv. Drug Delivery Rev.* **2007**, *59*, 1413.
[5] C. Burger, B. S. Hsiao, B. Chu, *Annu. Rev. Mater. Res.*, **2006**, *36*, 333.
[6] M. Goldberg, R. Langer, X. Q. Jia, *J. Biomater. Sci.-Polym. Ed.* **2007**, *18*, 241.
[7] D. Liang, B. S. Hsiao, B. Chu, *Adv. Drug Delivery Rev.* **2007**, *59*, 1392.
[8] S. Liao, C. K. Chan, S. Ramakrishna, *Mater. Sci. China* **2010**, *4*, 29.
[9] B. C. Kim, S. Nair, J. Kim, J. H. Kwak, J. W. Grate, S. H. Kim, M. B. Gu, *Nanotechnology* **2005**, *16*, S382.
[10] B. C. Kim, D. Lopez-Ferrer, S. M. Lee, H. K. Ahn, S. Nair, S. H. Kim, B. S. Kim, K. Petritis, D. G. Camp, J. W. Grate, R. D. Smith, Y. M. Koo, M. B. Gu, J. Kim, *Proteomics* **2009**, *9*, 1893.
[11] H. K. Ahn, B. C. Kim, S. H. Jun, M. S. Chang, D. Lopez-Ferrer, R. D. Smith, M. B. Gu, S. W. Lee, B. S. Kim, J. Kim, *Biotechnol. Bioeng.* **2010**, *107*, 917.
[12] S. Nair, J. Kim, B. Crawford, S. H. Kim, *Biomacromolecules* **2007**, *8*, 1266.
[13] S.-H. Jun, M. S. Chang, B. C. Kim, H. J. Ahn, D. Lopez-Ferrer, R. Zhao, R. D. Smith, S.-W. Lee, J. Kim, *Anal. Chem.* **2010**, *82*, 7828.
[14] N. N. Hunder, H. Wallen, J. H. Cao, D. W. Hendricks, J. Z. Reilly, R. Rodmyre, A. Jungbluth, S. Gnjatic, J. A. Thompson, C. Yee, *New Engl. J. Med.* **2008**, *358*, 2698.
[15] S. Jung, Y. K. Park, H. Lee, J. H. Shin, G. R. Lee, S. H. Park, *Exp. Mol. Med.* **2010**, *42*, 187.
[16] T. Manabe, K. Mizumoto, E. Nagai, K. Matsumoto, T. Nakamura, T. Nukiwa, M. Tanaka, T. Matsuda, *Clin. Cancer Res.* **2003**, *9*, 3158.
[17] C. A. Ellison, J. G. Gartner, *J. Immunol. Meth.* **1995**, *186*, 233.
[18] E. Parra, A. G. Wingren, G. Hedlund, T. Kalland, M. Dohlsten, *J. Immunol.* **1997**, *158*, 637.
[19] M. K. Majumdar, V. Banks, D. P. Peluso, E. A. Morris, *J. Cell. Physiol.* **2000**, *185*, 98.
[20] K. R. H. Brunt, S. R.; Ward, C. A.; Melo, L. G., *Meth. Mol. Med.* **2007**, *139*, 197.
[21] N. A. Moatamed, G. Nanjangud, R. Pucci, A. Lowe, I. P. Shintaku, S. Shapourifar-Tehrani, N. Rao, D. Y. Lu, S. K. Apple, *Am. J. Clin. Pathol.* **2011**, *136*, 754.
[22] D. Pils, A. Pinter, J. Reibenwein, A. Alfanz, P. Horak, B. C. Schmid, L. Hefler, R. Horvat, A. Reinthaller, R. Zeillinger, M. Krainer, *Br. J. Cancer* **2007**, *96*, 485.

[23] Y. Tang, L. Wang, P. Zhang, H. Wei, R. Gao, X. Liu, Y. Yu, *Clin. Vaccine Immunol.* **2010**, *17*, 1903.
[24] C. F. Qu, Y. Li, Y. J. Song, S. M. Rizvi, C. Raja, D. Zhang, J. Samra, R. Smith, A. C. Perkins, C. Apostolidis, B. J. Allen, *Br. J. Cancer* **2004**, *91*, 2086.
[25] M. E. Gomes, R. L. Reis, *Int. Mater. Rev.* **2004**, *49*, 261.
[26] J. Venugopal, M. P. Prabhakaran, S. Low, A. T. Choon, Y. Z. Zhang, G. Deepika, S. Ramakrishna, *Curr. Pharm. Design* **2008**, *14*, 2184.
[27] P. K. Smith, R. I. Krohn, G. T. Hermanson, A. K. Mallia, F. H. Gartner, M. D. Provenzano, E. K. Fujimoto, N. M. Goeke, B. J. Olson, D. C. Klenk, *Anal. Biochem.* **1985**, *150*, 76.